

# Thermally driven non-contact atomic force microscopy

Anil Gannepalli and Abu Sebastian

*NanoDynamics Systems Laboratory, Department of Electrical and Computer Engineering, Iowa State University, Ames, Iowa 50011*

Jason Cleveland

*Asylum Research, Santa Barbara, California 93117*

Murti Salapaka<sup>a)</sup>

*NanoDynamics Systems Laboratory, Department of Electrical and Computer Engineering, Iowa State University, Ames, Iowa 50011*

(Received 16 March 2005; accepted 13 July 2005; published online 6 September 2005)

In this letter a thermally driven frequency modulated atomic force microscopy (FM-AFM) technique is developed. Thermal fluctuations of the cantilever are employed to estimate the cantilever's equivalent resonant frequency. The corresponding cantilever oscillations are the smallest possible at a given temperature. Related experiments that establish the feasibility of thermally driven FM-AFM in ambient room conditions have achieved tip-sample separations less than 2 nm with long term separation stability ( $>30$  min). Employing this method a narrowband 250 Hz modulation of the tip-sample separation was detected with a vertical resolution of 0.25 Å in a 0.4 Hz bandwidth. The corresponding estimated force sensitivity is 7 fN. In all experiments the cantilever tip was maintained in the attractive regime of the tip-sample interactions. This demonstrates a thermally driven non-contact mode operation of AFM. It also provides a limits of performance study of small amplitude FM-AFM methods. © 2005 American Institute of Physics. [DOI: 10.1063/1.2037197]

In many studies a minimally invasive investigation of extremely small and local forces at room temperature utilizing a micro-cantilever is of significant interest. Relevant applications include non-invasive detection of cell wall motion<sup>1</sup> and single electron spin detection.<sup>2</sup> In such studies the detection of localized forces requires extremely small tip-sample separations that have to be maintained for extended periods of time. This requirement is either imposed by the time scales of the dynamic process being studied or the need to achieve the necessary sensitivity.

Classical non-contact methods with large amplitudes ( $A \approx 5\text{--}80$  nm) suffer from limited sensitivity to short-range forces and complex non-linear dependence of the resonance shifts on the tip-sample force gradients. Small amplitudes in the sub-Ångstrom regime are recommended<sup>3</sup> for improved sensitivity to short-range forces and ease of data interpretation. For such small amplitudes cantilever's resonance shift due to conservative tip-sample forces is accurately given by  $\Delta\omega_R \approx \omega_R(k_s/2k)$ , where  $\omega_R = \omega_0\sqrt{1-(1/4Q^2)}$  is the cantilever's resonance,  $\omega_0$  and  $Q$  are the undamped resonant frequency and quality factor of the cantilever,  $k_s$  is the local tip-sample force gradient and  $k$  is the cantilever's stiffness. Thus in small amplitude dynamic AFM methods data interpretation is straightforward. Small amplitude on-resonance amplitude modulation (AM)<sup>4</sup> and off-resonance AM<sup>5–8</sup> methods have been successfully demonstrated. Frequency modulation (FM) experiments<sup>9</sup> with 2.8 nm amplitudes in UHV have demonstrated atomic resolution of Si(111)-(7×7) surface at room temperature. However, amplitudes employed in<sup>9</sup> are still an order of magnitude larger than desirable. FM-AFM studies<sup>10</sup> with sub-nanometer amplitudes ( $\approx 8$  Å) and extremely stiff ( $k=1800$  N/m) cantilevers in UHV have imaged the subatomic features on the Si(111)-(7×7) surface.

Small amplitude methods require stiff cantilevers to avoid the jump-to-contact instability. At room temperature on-resonance small amplitude methods suffer from the operational difficulties of providing a stable small amplitude drive.<sup>11</sup> This issue is further aggravated in FM methods where the thermal vibrations corrupt the positive feedback drive. Off-resonance AM techniques or use of low  $Q$  cantilevers alleviate the problem of small drives while compromising the resonant enhancement to sensitivity. Stiffer cantilevers<sup>10</sup> also address the challenge of small drives but result in lower sensitivity.

This letter presents the thermally driven non-contact AFM method that falls in the small amplitude FM-AFM category. This FM method exploits<sup>12</sup> the thermal forcing of the cantilever, thereby obviating the external positive feedback excitation. Furthermore, the amplitudes realized in thermally driven FM-AFM are that of the thermal fluctuations of the cantilever and hence the smallest possible at a given temperature. Additionally, the broadband nature of the thermal forcing can potentially yield information at frequencies away from resonance. In FM-AFM the thermal limit to the minimum detectable frequency shift<sup>13</sup> is  $\delta\omega = \sqrt{k_B T B \omega_0 / k \langle A^2 \rangle Q}$ , where  $k_B$ ,  $T$ , and  $B$  are the Boltzmann constant, temperature and bandwidth respectively. With smaller amplitudes the frequency noise increases and in the limiting case ( $\langle A^2 \rangle \approx k_B T / k$ ), the frequency noise is  $\delta\omega = \sqrt{\omega_0 B / Q}$ . In such a case the temperature independence of frequency noise is potentially useful for applications requiring elevated temperatures. For the experiments reported in this letter with  $T=300$  K,  $Q=450$ ,  $k=1$  N/m,  $\omega_0=2\pi \cdot 350 \times 10^3$  rad/s the rms amplitude is  $\langle A^2 \rangle^{1/2} \approx 0.64$  Å and the theoretical frequency noise density is 489 Hz<sup>2</sup>/Hz. Such fundamentally large noise densities necessitate much smaller bandwidths compared to driven dynamic methods where the frequency noise is reduced by operating at low temperatures and/or

<sup>a)</sup>Electronic mail: murti@iastate.edu

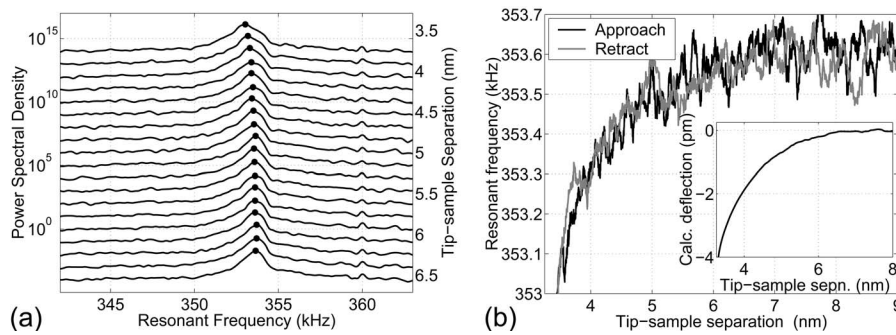


FIG. 1. (a) As the tip-sample separation decreases, the peak position shifts towards lower frequencies indicating increasingly attractive forces. (b) The corresponding variation observed in the frequency estimates during approach and retract phases of a force curve. Calculated deflection  $p_{\text{calc}} = (2/\omega_0) \int \Delta\omega_R dl$  for the observed frequency changes is shown in the inset. The maximum calculated deflection of 4 pm is much smaller than the deflection sensitivity ( $\approx 1 \text{ \AA}$ ) of the instrument at small frequencies.

with higher amplitudes. Stiffer cantilevers lead to smaller noise densities, however, the signal-to-noise ratio (SNR)  $\Delta\omega_R / \delta\omega \approx (k_s/2) \sqrt{Q\omega_0 \langle A^2 \rangle} / k_B k_B T$  decreases with stiffness for a given amplitude and temperature. Therefore as long as  $k + k_s > 0$ , it is advantageous to use a softer cantilever. Thermally driven FM-AFM enables the FM operation with smallest possible amplitudes at room temperature while employing cantilevers stiff enough to ensure mechanical stability. This is achieved by compromising bandwidth.

In thermally driven FM-AFM the information about the conservative and dissipative tip-sample interactions is available in the power spectrum of the cantilever's thermal fluctuations as the changes in the position and width of the spectral peak. A change in the effective resonant frequency  $\omega_{R,\text{eff}} (= \omega_R + \Delta\omega_R)$ , induced by the tip-sample interactions, is indicated by a shift in the peak position. For a high  $Q$  cantilever, the thermal noise response is assumed to be a single sinusoid in white noise. The frequency of this sinusoid, corresponding to the effective resonant frequency of the cantilever, is estimated by Pisarenko harmonic decomposition.<sup>14</sup>

The estimated frequency is fed back to the controller that compensates for the disturbances to maintain a desired effec-

tive resonant frequency. Consequently, the tip-sample separation  $l$  is controlled. The controller rejects disturbances that have a signal bandwidth less than the closed loop bandwidth. However, disturbances with frequency content greater than the closed loop bandwidth appear as changes in the cantilever's equivalent resonant frequency. The disturbances comprise of an undesirable part such as the drift effects that are slow and a desirable signal such as the changes in tip-sample forces. The controller is designed such that the closed loop serves to compensate for the effects of drift while recording the imaging signal in open loop. Therefore, this technique is particularly suited for room temperature applications where drift compensation is crucial and the changes in the tip-sample forces are persistent.

The thermal noise based non-contact mode operation was demonstrated in a variety of experiments few of which are discussed below. The experiments were performed on a digital instruments multimode AFM in ambient environment. Silicon cantilevers were used with freshly cleaved HOPG surface. The frequency noise density is  $\approx 600 \text{ Hz}^2/\text{Hz}$  that is near the theoretical limit of  $\approx 490 \text{ Hz}^2/\text{Hz}$  calculated assuming only thermal noise is the source of frequency estimation

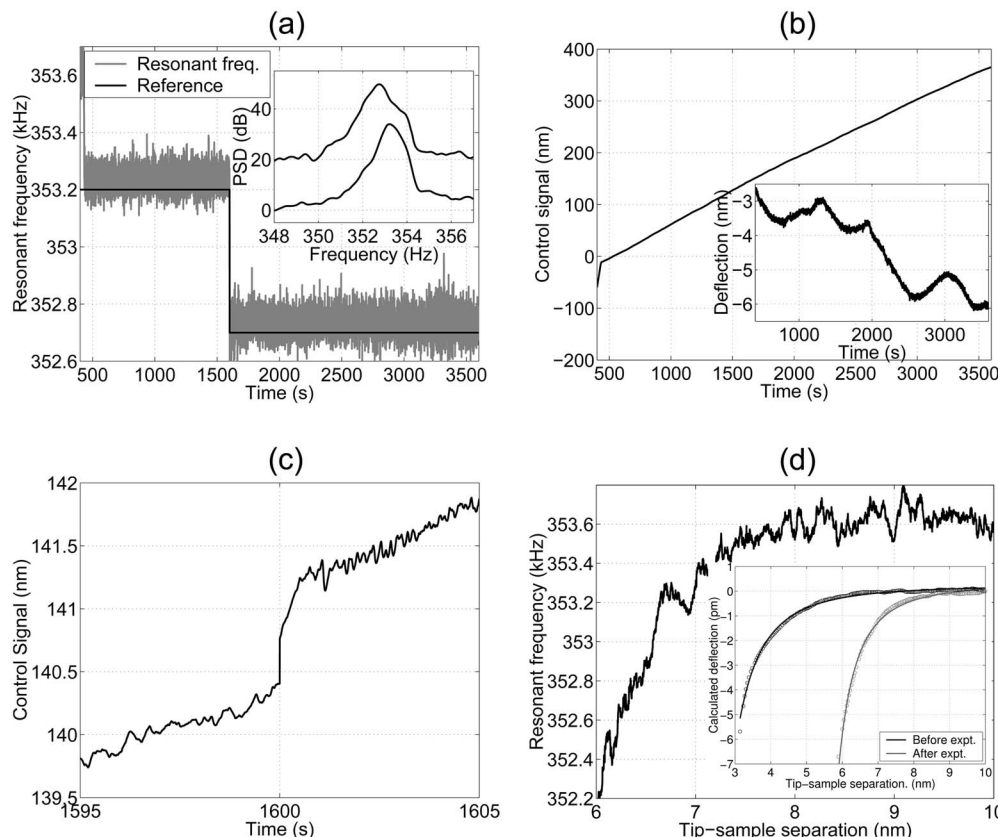


FIG. 2. (a) Time history of the estimated frequency (gray) while tracking a step change in the reference (black) at 1600 s. The shift in the peak position and peak width of the spectral density of the cantilever's thermal response before and after the step is apparent in the inset. (b) The controller acts predominantly to compensate for the drift in the system. The inset shows the changes in deflection due to the drift. (c) Controller responds to the step change in reference by reducing the tip-sample separation. (d) Updated dependence of the resonant frequency on the tip-sample separation. (Inset) calculated cantilever deflections  $p_{\text{calc}}$  before (black) and after (gray) the experiment are shown as circles. A van der Waals type force  $[p_{\text{calc}} \propto R_{\text{vdW}} \propto (l - l_0)^{-2} (l - l_0 + 2R)^{-2}]$  fit to the deflections is shown as solid lines. A value of 10 nm is used for the tip radius  $R$  and the resulting fits estimate the thickness of the adsorbed layer to be  $l_0 \approx 1.6 \text{ nm}$  at the beginning of the experiment. The thickness of this layer increases to  $l_0 \approx 4.9 \text{ nm}$  by the end of the hour long experiment. Therefore the true tip-sample separation is  $(l - l_0) \approx 1.4 \text{ nm}$  throughout the experiment.

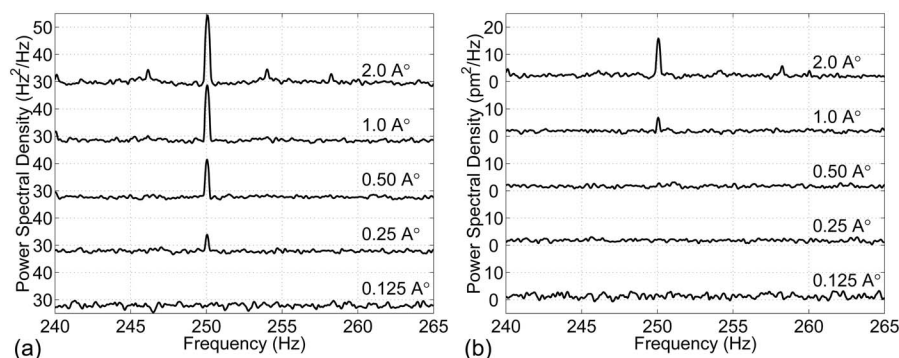


FIG. 3. Power spectral densities (in db) of the changes in the (a) resonant frequency (b) cantilever deflection for different amplitude modulations of the tip-sample separation  $l$  at 250 Hz. Higher sensitivity of cantilever's resonance to tip-sample forces is evident in (a) where modulations in  $l$  as small as 0.25 Å are detected. In comparison deflection signal does not register the modulations in  $l$  until the modulation amplitude is 1 Å.

error. The noise in the deflection sensor closes the gap even further. Thus the sensitivities achieved in the following experiments are reasonably close to the theoretical limits. In Fig. 1(b) it is seen that the resonant frequency decreases with decreasing tip-sample separation indicating increasing strength of attractive forces. A slight widening of the peak is also observed indicating an increased dissipation closer to the sample surface. The tip-sample forces cannot be detected by deflection as the maximum observable deflection (see inset in Fig. 1) is estimated to be approximately 4 pm that is much smaller than the deflection sensitivity of the instrument of  $\approx 1$  Å at low bandwidths.

The following experiment demonstrates the feasibility of the proposed method to control the tip-sample separation for extended time periods. The natural resonant frequency of the cantilever and the reference frequency to be tracked by the controller are 353.6 and 352.7 kHz, respectively [see Fig. 2(a)]. Once the desired tip-sample separation is achieved, indicated by the resonant frequency being close to the reference, the control action counteracts the drift in the instrument. The closed loop bandwidth, estimated to be about 1.4 Hz is sufficient for drift compensation. At approximately 1600 s into the experiment the step change in the reference is introduced. It is evident from Fig. 2(a) that the controller is able to track this change. As the reference frequency is reduced, implying a smaller desired tip-sample separation, the controller moves the sample towards the tip. This is seen as a small "jump" in the control effort [see Fig. 2(c)] at 1600 s. The new setpoint is reached in less than 1 s. As reasoned earlier, the variations in deflection in inset of Fig. 2(b) can be attributed to the drift in the deflection sensor as the tip-sample forces are too small to induce any perceivable change in the deflection.

At the end of the experiment the updated resonant frequency versus tip-sample distance is shown in Fig. 2(d). Note that the estimated separation of about 6.3 nm at 352.7 kHz is greater than the corresponding separation in Fig. 1(b). This discrepancy is attributed to the changes in the separation between the tip and HOPG surface due to the accumulation of adsorbates during the long duration of the experiment. True tip-sample separation is estimated by fitting a van der Waals type force to the observed force dependence on the tip-sample separation [see the inset in Fig. 2(d)]. The fits estimate the adsorbed layer thickness to increase from 1.6 to 4.9 nm during the experiment (2 nm thick layer was reported<sup>15</sup> at low humidities). This gives a separation of approximately 1.4 nm between the tip and adsorbed layer for 30 min.

Figure 3 demonstrates the non-contact imaging capability of this method where the sample position is modulated by 0.125–2 Å, 250 Hz sinusoids. The modulation frequency is

far above the closed-loop bandwidth of 1.4 Hz and thus the controller does not counteract the sample modulations. The controller, by effectively compensating for drift, tracks a reference frequency of 353.2 kHz that is less than the cantilever's natural resonance implying non-contact mode operation. The tip-HOPG surface separation is estimated to be approximately 4.2 nm. It is evident from the peaks of the power spectra in Fig. 3(a) that modulations as small as 0.25 Å are detectable by monitoring the cantilever's effective resonance. The peak width of the spectrum for 0.25 Å oscillations in Fig. 3(a) is approximately 0.4 Hz and the rms change in the resonant frequency  $\delta\omega_R$  estimated from the area under the peak is 35 Hz. Thus the force sensitivity  $\delta F_s = [(2k/\omega_R)\delta\omega_R\delta l]$  is 7 fN. The deflection signal does not register the sample movement [see Fig. 3(b)] until the modulations are as large as 1 Å. Thus the vertical resolution of resonant frequency is at least 4 times better than the vertical resolution of the deflection.

In this letter, a novel thermally driven non-contact mode of AFM operation is demonstrated. This FM method utilizes the thermal vibrations of the cantilever for non-contact mode operation with the smallest possible amplitude at a given temperature. This technique, therefore, is the limiting case of small amplitude FM-AFM methods.

M.S. acknowledges the support from the NSF Grant ECS-0330224.

<sup>1</sup>A. E. Pelling, S. Sehati, E. B. Gralla, J. S. Valentine, and J. K. Gimzewski, *Science* **305**, 1147 (2004).

<sup>2</sup>K. Holczer, *Development of a single electron spin microscope*, DARPA, MOSAIC Proposal (2001).

<sup>3</sup>H. Holscher, U. D. Schwarz, and R. Wisendanger, *Appl. Surf. Sci.* **140**, 344 (1999).

<sup>4</sup>R. Erlandsson and L. Olsson, *Appl. Phys. A: Mater. Sci. Process.* **66**, S879 (1998).

<sup>5</sup>P. M. Hoffmann, A. Oral, R. A. Grimble, H. O. Ozer, S. Jeffery, and J. B. Pethica, *Proc Royal Society London Series A*, **457**, 1161 (2001).

<sup>6</sup>S. P. Jarvis, M. A. Lantz, U. Durig, and H. Tokumoto, *Appl. Surf. Sci.* **140**, 309 (1999).

<sup>7</sup>S. P. Jarvis, H. Yamada, S. I. Yamamoto, H. Tokumoto, and J. B. Pethica, *Nature (London)* **384**, 247 (1996).

<sup>8</sup>A. Oral, R. A. Grimble, H. O. Ozer, P. M. Hoffmann, and J. B. Pethica, *Appl. Phys. Lett.* **79**, 1915 (2001).

<sup>9</sup>T. Eguchi and Y. Hasegawa, *Phys. Rev. Lett.* **89**, 266105 (2002).

<sup>10</sup>F. J. Giessibl, S. Hembacher, H. Bielefeldt, and J. Mannhart, *Science* **289**, 422 (2000).

<sup>11</sup>P. M. Hoffmann, *Dekker Encyclopedia of Nanoscience and Nanotechnology* (Marcel Dekker, 2004), p. 3641.

<sup>12</sup>F. J. Giessibl, *Jpn. J. Appl. Phys., Part 1* **33**, 3726 (1994).

<sup>13</sup>T. R. Albrecht, P. Grütter, D. Horne, and D. Rugar, *J. Appl. Phys.* **69**, 668 (1991).

<sup>14</sup>V. F. Pisarenko, *Geophys. J. R. Astron. Soc.* **33**, 347 (1973).

<sup>15</sup>S. P. Jarvis, A. Oral, T. P. Weihs, and J. B. Pethica, *Rev. Sci. Instrum.* **64**, 3515 (1993).